

# Feasibility Study of an Industrial Moisture Content Sensor Based on Wheeler Cap

Prakorn Pratoomma<sup>1,2</sup>, Abel Zandamela<sup>3</sup>, Suramate Chalermwisutkul<sup>1</sup>, Adam Narbudowicz<sup>3</sup>

<sup>1</sup>High Frequency Systems Laboratory, TGGs, King Mongkut's University of Technology North Bangkok, Thailand

<sup>2</sup>Defense Technology Institute, Nonthaburi, Thailand

<sup>3</sup>CONNECT Centre, Trinity College Dublin, Ireland

prakorn.p@dti.or.th, prakorn.p-ce2016@tggs.kmutnb.ac.th

**Abstract**— The paper proposes a technique for sensing of moisture content of a waste paper block based on Wheeler Cap measurement method. The technique allows sufficient penetration into the sample due to relatively low frequencies in the VHF band. Water blocks within the sample can be detected due to the increased loss compared to a dry sample. The simulation setup comprises a cylindrical Wheeler Cap structure and an electrically small antenna which is located in the same enclosure as the Material Under Test (MUT). The moisture content can be detected due to frequency shift and amplitude change of the reflected signal. The study demonstrates that varying moisture content from 5% to 50% results in the change of the frequency from 276.35 MHz to 264.35 MHz, and simultaneous change in the level of reflected signal from -4.51 to -6.64 dB. Other factors, such as misplacement of the sample, are also discussed.

**Index Terms**— Wheeler Cap, Electrically Small Antennas, Moisture Content Measurement, Folded Spherical Helix Antenna, Smart Industry, Green Technology.

## I. INTRODUCTION

The measurement of moisture content is a crucial process in multiple industrial applications, spanning from agricultural and food production to biomass and renewable energy. The latter application is relevant for incinerators or waste-to-energy power plants. Such plants burn certain types of waste to produce electric energy. However, the production is efficient only if the moisture content of burned waste is below 35 % [1].

Moisture content measurement methods can be categorized into two groups: direct and indirect. Direct methods are typically conducted in a well-controlled laboratory environment with a high level of precision [2]. Indirect methods are methods that can perform faster than the former. They are often sensitive to surroundings and require calibration. These methods include optical, dielectric (including rf-based techniques), and nuclear approaches [2]. For instance, near-infrared spectroscopy is an optical device for measuring and controlling the moisture content of the compost [3]. Microwave measurements are also used in many agricultural applications [4]. Nuclear magnetic resonance (NMR) measurements are generally accepted standards in pharmaceutical and food industries [5].

Several radio-based techniques are used to detect the dielectric properties of the Material Under Test (MUT) [4][6].

In [6], the cavity perturbation and the transmission line methods are suitable for measuring small-size, motionless samples enclosed in a cavity or in vicinity to a transmission line. For non-destructive, contactless material sensing, the free-space transmission technique can be used. At present, it is applicable to a high-temperature sample such as plasma [6].

Wheeler Cap is a cost-effective approach proposed by Harold A. Wheeler in 1959 for antenna efficiency measurements [7]. It is based on an equivalent circuit of an antenna, where radiation resistance and loss resistance can be represented as two serial components. If an antenna is fully surrounded by the cap, its radiation resistance becomes short-circuited. By comparing reflection coefficients between the antenna in free space and antenna in the cap, one can calculate antenna losses [7].

The paper proposes a new technique for moisture content measurement within a large volume of MUT based on modified Wheeler Cap technique. Since water has a loss tangent of 1.832 at 200 MHz (see Figure 4.), it is expected to generate losses when placed inside the cap. By measuring the reflection coefficient, one can measure moisture content in the MUT, i.e. whether the 35% threshold for the energy production in an incinerator was reached. The use of relatively low frequencies in the VHF band allows sufficient penetration of electromagnetic fields into the 10 cm x 10 cm x 10 cm sample block, as processed in incinerator plants. This paper reports the initial feasibility study of such a sensor, based on simulations with CST Microwave Studio. Preliminary results suggest that this type of sensor is suitable to distinguish different moisture contents with the required accuracy. While it identifies some sources of a possible discrepancy, it is assessed that those can be controlled by a proper antenna and cap design.

## II. PURPOSED MEASUREMENT SETUP

The system was modeled in CST Microwave Studio and simulated using the frequency-domain solver. Investigated frequencies range from 200 MHz ( $\lambda_0 = 149.89$  cm) and 350 MHz ( $\lambda_0 = 85.65$  cm). The coaxial waveguide port is

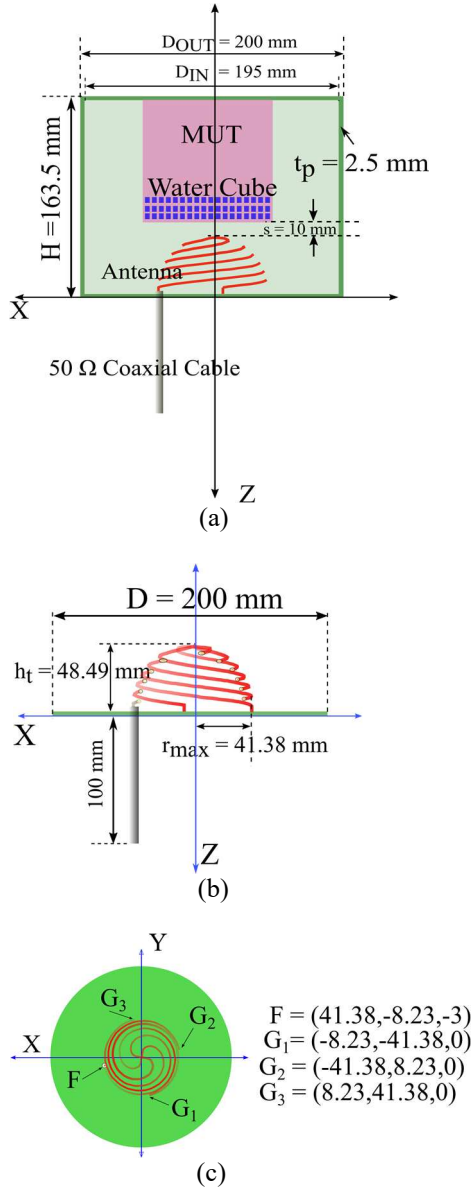


Fig. 1. Proposed systems: (a) side view of the complete system; (b) side view of the antenna; (c) top view of the antenna with coordinates of the feeding point (F) and three grounding points (G1, G2, G3)

assigned at one end of the 50  $\Omega$  coaxial cable, and  $S_{11}$  and the field distribution are calculated and recorded during the solver run.

A cylindrical conducting cap made of Perfect Electric Conductor (PEC) is used. The measurement setup is shown in Fig. 1a. Its total height is  $H = 163.5$  mm, outer diameter  $D_{OUT} = 200$  mm, inner diameter  $D_{IN} = 195$  mm, and cylindrical wall thickness  $t_p = 2.5$  mm. The radius of the cap (97.5 mm) is less than radian length ( $\lambda/2\pi$ ), satisfying size conditions proposed by Harrington in [7] ( $\lambda/2\pi$  being 238.6 mm at 200 MHz and 136.3 mm at 350 MHz). Contrary to the original concept, this work aims to find the change in the reflection coefficient caused by the additional losses due to moisture. In this context, the condition of  $D_{IN} < \lambda\pi$  is required to avoid

resonant modes in the cavity, which alter electric field distribution.

As the size of the cap needs to be sufficiently small, an electrically small antenna is required. A one-turn four-arm folded helix antenna proposed by S. Best in [9], is implemented. The design offers substantial miniaturization while preserving low losses and relatively low Q factor with  $Q = 32$  and a high efficiency of 98.6%. Additionally, the metal-only design offers a sturdy structure for implementation in an industrial set-up. The antenna is designed according to guidelines in [9]. Its details are shown in Fig. 1 (b) with the following dimensions: wire diameter 2.6 mm, total antenna height  $h_t = 48.49$  mm, and maximum spherical radius  $r_{max} = 41.38$  mm. The antenna comprises of four arms, which climb along a semi-spherical plane, each making one full turn before reaching the top of the semi-sphere [9]. Three of the arms are grounded, while the fourth one is connected to the inner wire of a coaxial cable. The antenna's semi-sphere protrudes from the cylindrical ground-plane at the bottom of the cap.

To ensure impedance matching with the 50- $\Omega$  coaxial cable, the L matching circuit [8] was used with a parallel capacitance of 9.47 pF and a series inductance of 25.548 nH. The antenna was designed to be best matched at 310 MHz in free space, as shown in Fig. 2.

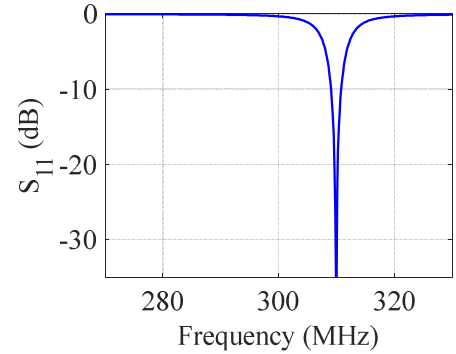


Fig. 2. Simulated  $S_{11}$  of the folded helix antenna used in the study.

The electric field distribution inside the cap is shown in Fig.3. Looking at the cut-plane at  $Y=0$ , the electric field is strongest in antenna proximity. This suggests that MUT should be placed around this area to get a maximum sensitivity. This is confirmed by the results described in Section IV.

The reflection coefficient ( $\Gamma$ ), when neither the cap nor MUT is present, can be calculated as:

$$\Gamma = Re \left\{ \frac{((R_{rad} + R_{loss}) - R_o)}{((R_{rad} + R_{loss}) + R_o)} \right\} \quad (1)$$

where  $R_{rad}$  is radiation resistance and  $R_{loss}$  is the antenna loss resistance. When the cap and MUT are present, (1) can be rewritten as:

$$\Gamma = Re \left\{ \frac{((R_{MUT} + R_{loss}) - R_o)}{((R_{MUT} + R_{loss}) + R_o)} \right\} \quad (2)$$

$R_{MUT}$  is the loss associated with losses in MUT. Since antenna loss  $R_{loss}$  is constant, it can be calibrated out of the equation leaving:

$$R_{MUT} = \frac{R_o(1+\Gamma)}{(1-\Gamma)} \quad (3)$$

which demonstrates the link between losses in MUT and the reflection coefficient.

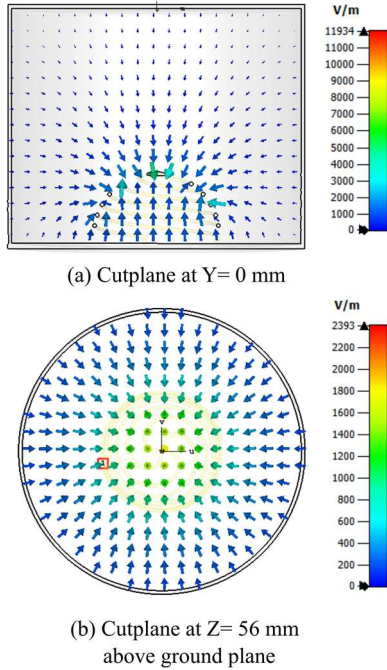


Fig. 3. Electric field distribution within the cap at 300 MHz.

### III. SIMULATION METHODOLOGY

The material under this investigation is a mixture of paper and water. The losses due to a proportion of water in the paper can be modeled using similar techniques described in [10][11] to obtain the complex dielectric constant (CDC) of the mixture. For accuracy, the model must be compared with the experimental data which are not available at this stage. To introduce the losses, a certain quantity of water cubes is inserted into the MUT instead.

The waste paper block (MUT) consists mostly of paper that is packed into a regular block of  $10\text{ cm} \times 10\text{ cm} \times 10\text{ cm}$ . This is in accordance with the guidelines of our industrial partner. The paper is defined as a lossless material and has a relative permittivity of  $\epsilon_{rp} = 2.31$ . The relative permittivity of water is set to  $\epsilon_{rw} = 78$ , and conductivity set to  $\sigma_w = 1.59\text{ S/m}$ . According to these values, the calculated loss tangent is shown in Fig.4. Those values are beneficial for the proposed application, as there is a strong contrast between the two materials.

In addition to water, losses are also introduced in the antenna, inner conductor, and insulation layer of the coaxial cable. Copper with an electric conductivity of  $\sigma_w = 5.7 \times 10^7$

S/m is defined as material of both the antenna and inner conductor of the cable. PTFE is used as the insulation layer of the cable and has a relative permittivity of  $\epsilon_{r\_ptfe} = 2.1$  and  $\tan\delta$  from the first-order Debye model with  $\tan\delta=0.0002@10\text{GHz}$ . Nevertheless, losses from copper and PTFE are less significant as the percentage of water increased. At 20% moisture content, loss due to water accounts for 36.54 % of total loss compared to 4.64 % of losses existed in both materials. This ratio is widening as the percentage of water increases. For instance, the ratio of loss from the water to the losses from copper and Teflon is 47.54 % to 4.18% at 45 percent of moisture content. In addition, the losses due to antenna and cable are constant, so they can be calibrated-out of the measurement system.

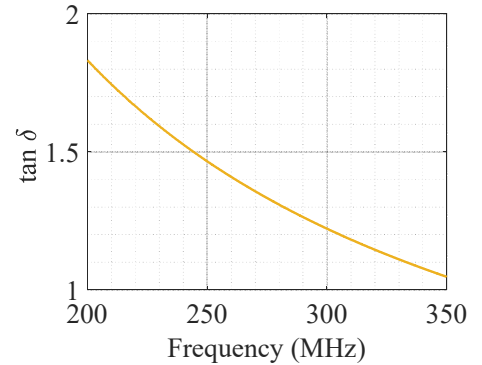


Fig. 4. Calculated loss tangent of water

Pockets of water are simulated as small cubical structures scattered across the MUT. Two sizes were investigated to assess the robustness of the simulation method: a 10-mm water cubes with 2 mm separation between neighboring cubes and a 5-mm water cubes with 0.5 mm separation. Fig.5 shows a comparison between the two sizes of water pockets for the exemplary cases of 15% and 40% moisture content. Both approaches resulted in similar frequency shift and minor discrepancy in the level of the reflected signal for 40% moisture. The later is attributed to numerical errors, i.e. different meshing between the two cases. The smaller water cubes of 5-mm will be used in the remainder of this paper.

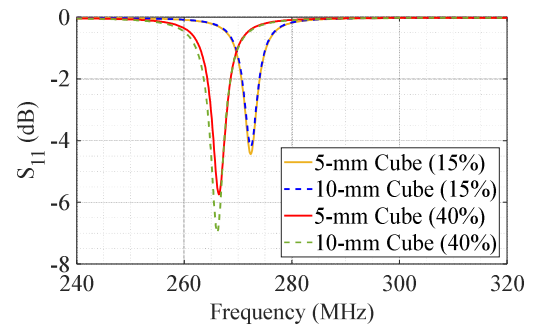


Fig. 5.  $S_{11}$  comparison of 5-mm water cube and 10-mm water cube.

The percentage of moisture content  $M_c$  is defined with respect to mass:

$$M_c = \frac{M_w}{(M_w + M_s)} \times 100\% \quad (4)$$

where  $M_s$  is a mass of the solid (here paper), and  $M_w$  is the mass of water. However, for the full-wave simulations, it is more convenient to control the volume. Based on known  $M_c$ , then (4) is rearranged to calculate the volume of water as:

$$V_w = \frac{V_T}{\rho_w \rho_{w1}} \quad (5)$$

$$\rho_{w1} = \frac{1}{\rho_w} + \frac{(100 - M_c)}{M_c \rho_s} \quad (6)$$

where  $\rho_w, \rho_s$ , and  $V_T$  are respectively the density of water (1000 kg/m<sup>3</sup>), the density of solid paper (800 kg/m<sup>3</sup>), and the total volume of MUT (1000 cm<sup>3</sup>). Based on  $V_w$ , the number of water cubes inserted into MUT is calculated.

#### IV. SIMULATION RESULTS

##### A. Detecting Changes in Moisture Content

The initial simulation examines whether the proposed method can distinguish between various moisture contents. The water cubes are placed near the bottom of the MUT (See Fig.1 (a)). The moisture content  $M_c$  is varied from 0 % to 50 % in 5 percentage point steps and the results of  $S_{11}$  are plotted in Fig.6. It can be seen that the resonant frequency gradually shifts downwards when  $M_c$  is increased. The minimum of  $S_{11}$  also decreases, which is in accordance with (3).

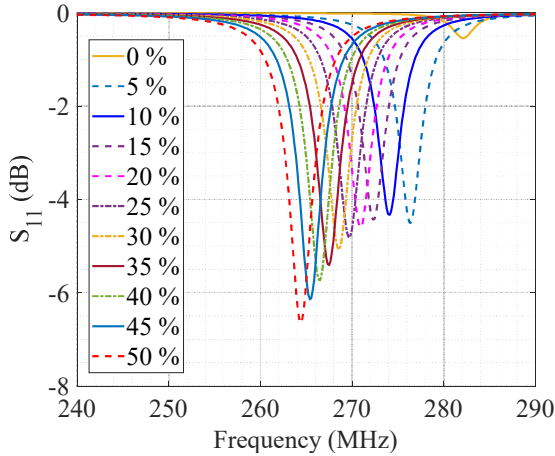


Fig. 6.  $S_{11}$  of the simulated system for different values of moisture content  $M_c$ .

Fig. 7 (a) and (b) show respectively the frequency of minimum  $S_{11}$  and its level at this frequency. Fig.7 (a) shows a linear relation between %  $M_c$  and resonant frequency. Both plots show almost a linear relationship for  $M_c > 10$  %.

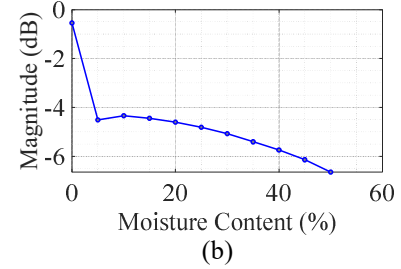
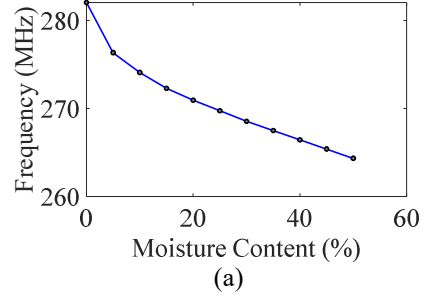


Fig. 7. (a) Resonant frequency over  $M_c$  (b) Magnitude (dB) over  $M_c$

##### B. Impact of MUT displacement

Three different locations of MUT block are considered, when the block is displaced 20 mm to the left (position A), central (position B) and displaced 30 mm to the right (position C). The locations are visualized in Fig.8 (a). Fig.8 (b) shows results for  $M_c = 40$  %. The result demonstrates the technique is not fully immune to the MUT displacement. However, this problem can be solved by appropriate mechanical design, which will prevent the displacement of the block.

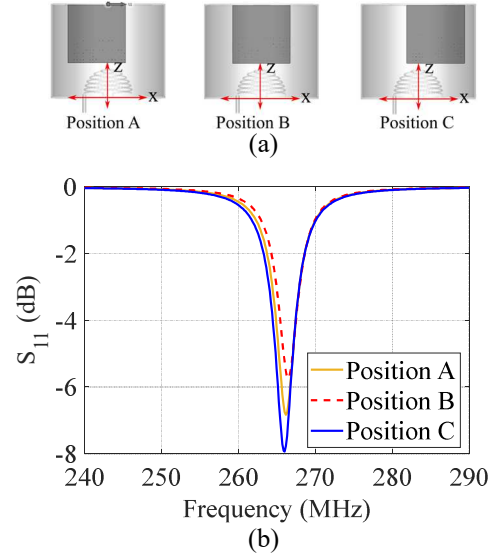


Fig. 8. (a) Three investigated location of the MUT (b)  $S_{11}$  for different MUT locations

### C. Impact of Water Content Displacement

The impact of the location of water cubes was studied, comparing the effects of moisture content present at the top and bottom parts of the MUT, as indicated in Fig. 9 (a). Both shown cases involve  $M_c = 25\%$  and  $50\%$ . The results are plotted in Figure 9. (b). For  $M_c = 25\%$ , a significant difference ( $-3.68$  dB) can be seen between the two cases. This can be explained as in location 2 the water is further away from the antenna, therefore having weaker interaction with the produced electric field (see electric field plot in Fig. 3). For location 1, the moisture content can still be detected based on  $S_{11}$ , however – as less energy interacts with the sample – the accuracy of the measurement deteriorates.

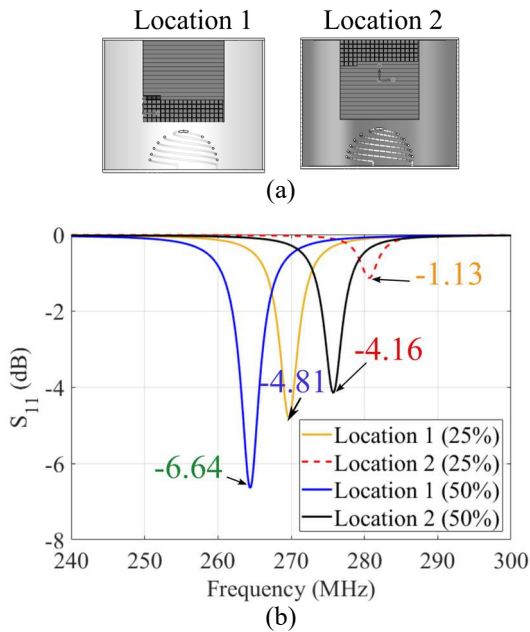


Fig. 9 Water content displacement (a) different locations of the water cubes (b)  $S_{11}$  for investigated.

### V. CONCLUSION

The paper proposes a technique that uses Wheeler Cap as a volumetric moisture sensor for industrial applications. The development was indented for the particular use case in an incinerator power plant, to assess whether the moisture content is below the 35% threshold required for its efficiency. Contrary to current technique, the method can assess large volumes of material, penetrating through the sample due to the relatively low VHF frequencies. Preliminary studies show that the technique can be employed as a moisture sensor for homogenous waste such as paper. Identified challenges can be solved by a proper mechanical design of the sensor.

### ACKNOWLEDGMENT

This work has been supported by a Research and Researchers for Industries (RRi) PhD Scholarship awarded by the National Research Council of Thailand: NRCT with the contract number PHD59I0033 and King Mongkut's University of Technology North Bangkok, Contract no.

KMUTNB-64-DRIVE-40, as well as Science Foundation Ireland grants no. 18/SIRG/5612 and 13/RC/2077.

### REFERENCES

- [1] J. Nithikul, "Potential of Refuse Derived Fuel Production from Bangkok Municipal Solid Waste," M.S. thesis, SERD, AIT, Thailand, 2007. Accessed on: Oct. 8, 2020. [Online]. Available: <http://faculty.ait.ac.th/visu/wp-content/uploads/sites/7/2019/01/Jidapa-Thesis-12-12-07.pdf>
- [2] M. V. Zambrano, B. Dutta, D. G. Mercer, H. L. Maclean, M. F. Touchie, "Assessment of moisture content measurement methods of dried food products in small-scale operations in developing countries: A review," *Trends in Food Science & Technology*, vol. 88, p. 484-496, June 2019. Available: <http://www.sciencedirect.com/science/article/pii/S0924224418304898>. [Accessed October 9, 2020].
- [3] K. Suehara, Y. Ohta, Y. Nakano, T. Yano, "Rapid measurement and control of the moisture content of compost using near-infrared spectroscopy," *Journal of Bioscience and Bioengineering*, vol. 87, No. 6, pp. 767-774, June 1999. Available: <http://www.sciencedirect.com/science/article/pii/S1389172399801510>. [Accessed Oct. 14, 2020].
- [4] S. Nelson, "Fundamentals of Dielectric Properties Measurements and Agricultural Applications," *The Journal of microwave power and electromagnetic energy: a publication of the International Microwave Power Institute*, pp. 98-113. Available: [https://www.researchgate.net/publication/51459698\\_Fundamentals\\_of\\_Dielectric\\_Properties\\_Measurements\\_and\\_Agricultural\\_Applications](https://www.researchgate.net/publication/51459698_Fundamentals_of_Dielectric_Properties_Measurements_and_Agricultural_Applications). [Accessed Sept. 30, 2020].
- [5] R. Wernecke, J. Wernecke, (2014). "Industrial moisture and humidity measurement: A practical guide,". Weinheim, Germany: Wiley-VCH, 2014, pp. 57-158. [Online] Available: [https://www.researchgate.net/publication/267376137\\_Industrial\\_Moisture\\_and\\_Humidity\\_Measurement\\_A\\_Practical\\_Guide/citations](https://www.researchgate.net/publication/267376137_Industrial_Moisture_and_Humidity_Measurement_A_Practical_Guide/citations). [Accessed Oct. 12, 2020].
- [6] Venkatesh, M. S., & Raghavan, G. S. V. (2005), "An overview of dielectric properties measuring techniques," *Canadian biosystems engineering*, 47(7), pp. 15-30. [Online] Available: [https://www.Researchgate.net/publication/235435108\\_An\\_Overview\\_of\\_Dielectric\\_Properties\\_Measuring\\_Techniques](https://www.Researchgate.net/publication/235435108_An_Overview_of_Dielectric_Properties_Measuring_Techniques). [Accessed Sept. 30, 2020].
- [7] H. A. Wheeler, "The Radiansphere around a Small Antenna," in *Proceedings of the IRE*, vol. 47, no. 8, pp. 1325-1331, Aug. 1959, doi: 10.1109/JRPROC.1959.287198.
- [8] Pozar, "David M. Microwave Engineering,". Hoboken, 3<sup>rd</sup> ed. NJ: Wiley, 2012. pp. 228-234, 719.
- [9] S. R. Best, "The radiation properties of electrically small folded spherical helix antennas," in *IEEE Transactions on Antennas and Propagation*, vol. 52, no. 4, pp. 953-960, April 2004, doi: 10.1109/TAP.2004.825799.
- [10] Jin, X.; Yang, W.; Gao, X.; Li, Z. "Analysis and Modeling of the Complex Dielectric Constant of Bound Water with Application in Soil Microwave Remote Sensing." *Remote Sensing*, vol. 12, issue 21, October 2020, 3544. <https://doi.org/10.3390/rs12213544>
- [11] D.A. Boyarskii, V.V. Tikhonov & N. Yu. Komarova (2002), "Model of Dielectric Constant of Bound Water in Soil for Applications of Microwave Remote Sensing - Abstract," *Journal of Electromagnetic Waves and Applications*, 16:3, 411-412, DOI: 10.1163/156939302-X01227